

LOAD OF THE HYDROSTATIC SLIPPER IN AXIAL PISTON PUMPS

Tadeusz Zloto, Konrad Kowalski

Institute of Machine Technology and Production Automation
Częstochowa University of Technology

Summary. The paper presents an analysis of the load of hydrostatic slippers in axial piston machines and describes the load of the basic mating surfaces. The hydrostatic load and relief of the slipper was studied with reference to the fundamental mathematical relationships. The results of simulation calculations of the slipper's twisting moment during its operation depending on the angular velocity, working pressure of the slipper's mass, and the coefficient of friction occurring between the swash plate in the pressure zone of the pump were obtained in the MathCad software. Their graphic representations are also shown.

Key words: piston pump, hydrostatic slipper, twisting moment.

INTRODUCTION

The reliability and durability of volumetric hydraulic piston machines crucially hinges on the condition of hydrostatic supports. Under the normal operating conditions the hydrostatic slipper should 'float', i.e. the fluid friction conditions should occur in the gap between the slipper and the swash plate, which takes over the load. The hydrostatic slipper in axial piston machines is of relatively small size and transfers large loads in demanding conditions. The swash plate is inclined at a certain angle with respect to the piston axis. The fact that the piston load is located off the axis, the presence of friction and inertia load can turn the slipper over.

No satisfactory mathematical model of the whole process of designing hydrostatic slippers has been developed so far. Manufacturers of hydraulic pumps must therefore rely on laborious experimental studies, assuming some kind of a trade-off between losses resulting from leakages and the slipper's wear-out [Brzuchowski, Kertynska and Kraszewski 1974, Osiecki L. 1998, Renius 1973]. The increasing demand for new types of pumps and for improving their performance necessitates developing universal and reliable constructions of high efficiency.

SLIPPER'S LOAD IN AN AXIAL PISTON PUMP

Fig. 1 presents the load of an axial piston pump. The force F_p coming from the pressure in the cylinder block acts upon the front surface of the piston. The dynamic force F_a acts upon the

piston system of the mass m_c (of the piston and slipper). The force F_a depends on the linear acceleration and mass of the piston system. The friction force F_T acts against the reciprocating movement of the piston, the directions of the two are opposite.

The normal force of the piston acts upon the slipper. The magnitude of the force is:

$$F_N = \frac{0.25\pi \cdot d^2 \cdot p_1 + F_T + F_{spr} + m_c \omega^2 r_p \tan \alpha \cos \varphi}{\cos \alpha}, \quad (1)$$

where:

- p_1 – the pressure in the cylinder block,
- F_{spr} – the force of the spring pressing the slipper,
- F_T – the friction force between the piston and the cylinder,
- m_c – the mass of the piston system,
- r_p – the radius of cylinder distribution in the cylinder block,
- α – the swash plate inclination angle,
- φ – the current angle of the cylinder block rotation .

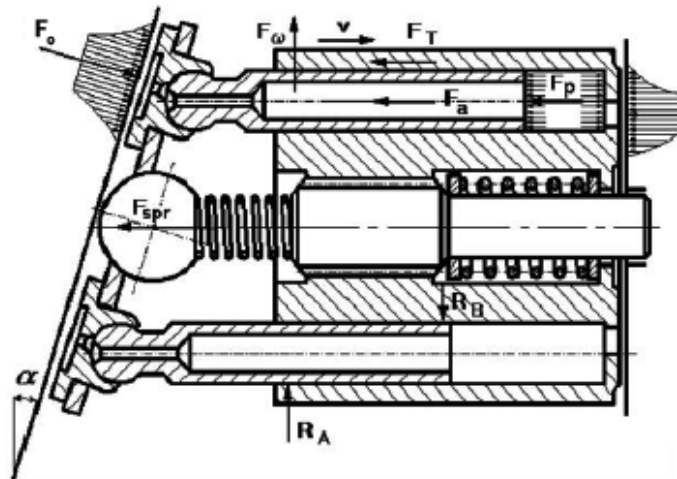


Fig. 1. Load of an axial piston pump

When a specific model (continuous or discrete) of the piston load and the friction coefficient μ_f are assumed, it is possible to find the reactive forces (Fig. 1) and friction occurring between the piston and the cylinder in accordance with [Kogal 1995, Osiecki A. 1998, Stryczek 1995]:

$$F_T = \mu_f (R_A + R_B). \quad (2)$$

HYDROSTATIC RELIEF OF THE SLIPPER

The slipper performs the task of transferring all the axial forces acting upon the piston system, and it is desirable to minimize energy losses and wear-out, and to maximize reliability within the full range of the pump operating parameters [Balas 1976, Osiecki A. and Osiecki L. 1998, Osiecki,

Niegoda 1976]. The slipper surface can have various shapes [Jerszow 1974, Jerszow B., Hiljuta and Jerszow Sz. 1993]. Regardless of the shape, there should be a central neck connecting the slipper with the piston pressure chamber.

In every typical slipper (Fig.2) an internal and external radius can be distinguished. The geometrical parameters of the slipper should be selected in such a way that the load carrying force resulting from the hydrostatic pressure field takes over 90 – 95 % of the normal load and the hydrodynamic force takes over the other 5 – 10 % of the load [Baszta 1971]. In the derivation of the formula for the pressure change on the slipper sealing surface it is assumed that the mating surfaces are smooth, the flow is laminar and isothermal. The pressure change in a typical slipper is:

$$p = p_o \frac{\ln \frac{r_2}{r}}{\ln \frac{r_2}{r_1}}, \quad (3)$$

where:

p, p_o - the pressures along the slipper radius and in the slipper chamber, respectively,
 r_2, r, r_1 - the external, current, and internal radius of the slipper, respectively.

The repulsive force of a typical hydrostatic slipper is [Szydelski, Olechowicz 1986]:

$$F_o = p_o \frac{\pi}{2} \cdot \frac{r_2^2 - r_1^2}{\ln \frac{r_2}{r_1}}. \quad (4)$$

The slipper construction affects power losses. The total power loss consists of the power lost due to leakage and friction loss. The crucial parameter is the gap height h_s (Fig. 2). With the increase in h_s the mechanical losses decrease, the volumetric losses, however, dramatically increase. Mechanical losses can be reduced by reducing the surfaces surrounding the gap. Slippers with additional bearing surfaces also contribute to minimizing mechanical losses by enabling significant hydrodynamic effects on a flat surface [Baszta, Zajczenko 1969, Lachner 1974].

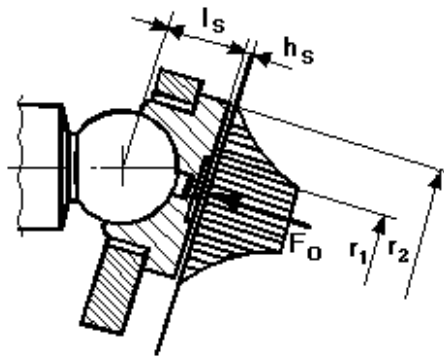


Fig. 2. Hydrostatic relief of the slipper

It is more difficult to design an axial piston pump of variable yield, in which it is necessary to transfer variable loads, resulting from the changes in the inclination angle α of the swash plate.

RESULTS OF THE SIMULATIONS OF THE SLIPPER LOAD

The twisting moment of the slipper was calculated for the pump of the typical dimensions and rated parameters as of those produced in Poland ($p_{nom} = 32$ MPa, $Q = 45$ l/min, $n_{nom} = 1500$ rotations/min). In the calculation model of the twisting moment, friction occurring between the slipper and the swash plate and centrifugal inertia force of the slipper were taken into consideration. The friction was obtained as a product of the force pressing the slipper towards the swash plate (obtained, in turn, as the difference of the normal force coming from the piston and the slipper hydrostatic relief) and the friction coefficient μ_s . The value of the friction coefficient was established empirically as $\mu_s = 0,003$ [Niegoda 1977]. It was assumed that the pressure drop between the cylinder and the slipper operating chamber was 10 % ($C_p = 0.9$) [Ivantysyn J. and Ivantysynova M. 2001].

The value of friction was obtained as:

$$F_{TS} = \mu_s \left[\frac{0.25\pi d^2 p_1 + F_T + F_{spr} + m_c \omega^2 r_p \operatorname{tg} \alpha \cos \varphi}{\cos \alpha} - C_p \frac{\pi p_1}{2} \left(\frac{r_2^2 - r_1^2}{\ln \frac{r_2}{r_1}} \right) \right], \quad (5)$$

and the value of the centrifugal inertia force of the slipper as:

$$F_{os} = m_s \left(\frac{\omega \cos \alpha}{\cos^2 \varphi + \cos^2 \alpha \cdot \sin^2 \varphi} \right)^2 \cdot r_p \sqrt{1 + \operatorname{tg}^2 \alpha \cos^2 \varphi}. \quad (6)$$

The resultant force acting upon the slipper was obtained as a geometrical sum of the projections of the component forces in the set of coordinates xy :

$$F_W = \sqrt{F_{WX}^2 + F_{WY}^2}. \quad (7)$$

After substituting and bringing the inertia force onto the plane on which the slipper and the swash plate mate:

$$F_W = \sqrt{\left(-F_{TS} \cos \varphi + F_{os} \cdot \frac{l_s}{l_{sc}} \sin \varphi \right)^2 + \left(F_{TS} \sin \varphi + F_{os} \cdot \frac{l_s}{l_{sc}} \cos \varphi \right)^2}. \quad (8)$$

where:

l_s – the distance between the coupling centre and the mating surface,

l_{sc} – the distance between the gravity centre and the mating surface.

The slipper's twisting moment is:

$$M_S = l_s \left\{ \begin{array}{l} -\mu_s \left[\frac{0.25\pi d^2 p_1 + F_T + m_c \omega^2 r_p \operatorname{tg} \alpha \cos \varphi}{\cos \alpha} - C_p \frac{\pi p_1}{2} \left(\frac{r_2^2 - r_1^2}{\ln \frac{r_2}{r_1}} \right) \right] \cos \varphi + \\ + m_s \left(\frac{\omega \cos \alpha}{\cos^2 \varphi + \cos^2 \alpha \cdot \sin^2 \varphi} \right)^2 r_p \sqrt{\operatorname{tg}^2 \alpha \cdot \cos^2 \varphi + 1} \frac{l_{sc}}{l_s} \sin \varphi \\ + \mu_s \left[\frac{0.25\pi d^2 p_1 + F_T + m_c \omega^2 r_p \operatorname{tg} \alpha \cos \varphi}{\cos \alpha} - C_p \frac{\pi p_1}{2} \left(\frac{r_2 - r_1}{\ln \frac{r_2}{r_1}} \right) \right] \sin \varphi + \\ + m_s \left(\frac{\omega \cos \alpha}{\cos^2 \varphi + \cos^2 \alpha \cdot \sin^2 \varphi} \right)^2 r_p \sqrt{\operatorname{tg}^2 \alpha \cdot \cos^2 \varphi + 1} \frac{l_{sc}}{l_s} \cos \varphi \end{array} \right. \quad (9)$$

In Eq. (9) the variable friction F_T being a function of the cylinder block rotation angle and occurring between the piston and the cylinder was calculated on the basis of a newly developed simulation model, which will be discussed in detail in subsequent publications.

Fig. 3 presents the dependence of the slipper twisting moment on the angular velocity of the cylinder block for the pressure zone.

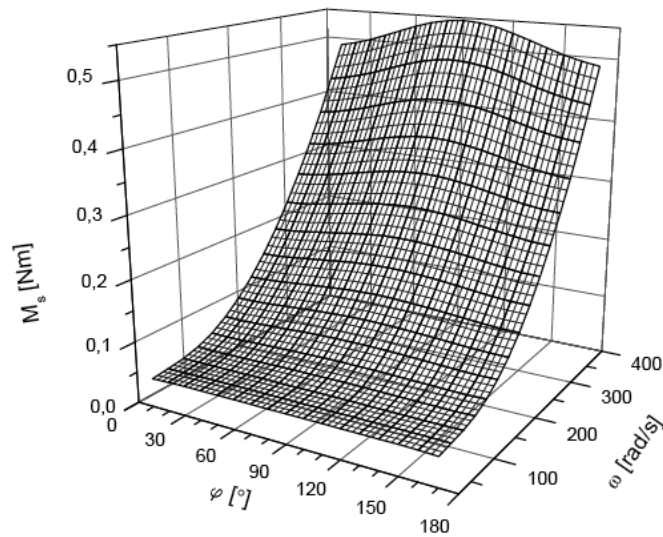


Fig. 3. Twisting moment of the slipper as a function of the angular velocity of the cylinder block for the pressure zone

As can be seen in Fig. 3, the influence of the angular velocity ω on the slipper twisting moment M_s is significant. Fig. 4 shows that the impact of the pressure on the twisting moment of the slipper is insignificant.

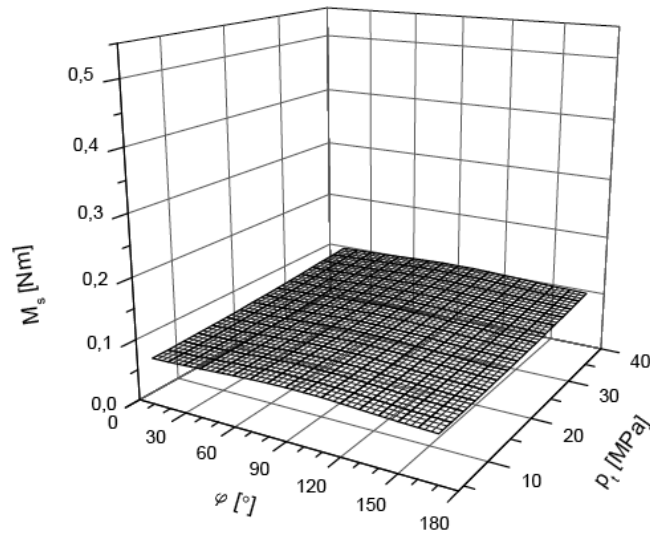


Fig. 4. Values of the slipper twisting moment depending on the pressure in the pressure zone

Fig. 5 shows values of the twisting moment depending on the slipper mass. For pressures zone, changes in the slipper mass affect the value of the twisting moment significantly.

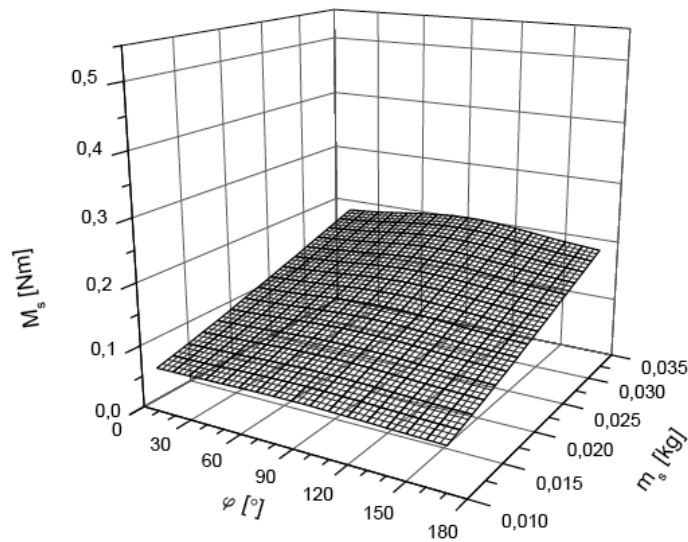


Fig. 5. Values of the twisting moment depending on the slipper mass for the pressure zone

In Fig. 6 the values of the slipper twisting moment are presented as a function of the friction coefficient for friction occurring between the slipper and the swash plate.

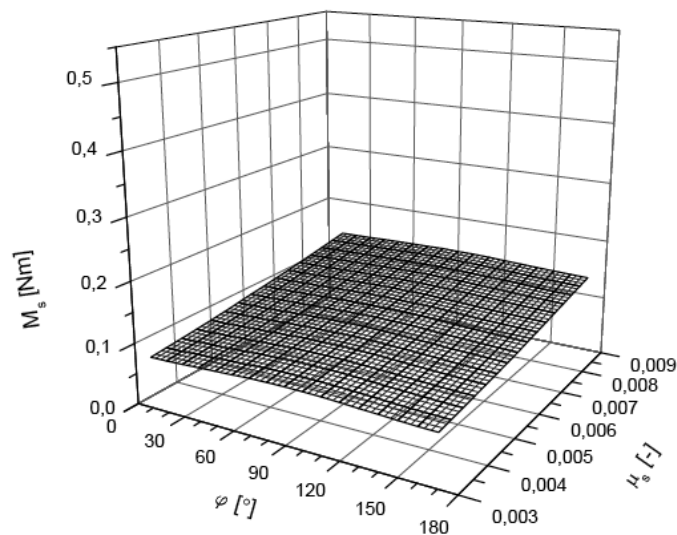


Fig. 6. Values of the slipper twisting moment depending on the friction coefficient for friction occurring between the slipper and the swash plate in the pressure zone

It can be observed that the friction coefficient affects the twisting moment significantly. The other construction parameters, such as the piston system mass, the spring pressing force, or exploitation parameters, such as the swash plate inclination angle, or friction between the piston and cylinder only slightly affect the value of the twisting moment.

CONCLUSIONS

The following conclusions can be formulated on the basis of the study:

- the decisive factor affecting the value of the twisting moment is the angular velocity of the cylinder block,
- the calculation model employed in the study is adequate for determining the influence of the basic construction and exploitation parameters of the pump on the slipper twisting moment,
- the accuracy of the twisting moment value obtained in the calculations crucially depends on friction occurring between the slipper and the swash plate. The relevant friction coefficient can be obtained only empirically.

REFERENCES

1. Balas W., 1976: Łożyska hydrostatyczne w osiowych pompach tłokowych. Przegląd Mechaniczny, nr 11.

2. Baszta T. M., 1971: Maszynostroitel'naja gidrawlika. Maszynostrojenie, Moskwa.
3. Baszta T.M., Zajczienko I. Z. 1969: Objemnyje gidrawliczeskije priwody. Maszynostrojenie, Moskwa.
4. Brzuchowski E., Kertyńska H., Kraszewski D., 1974: Wyniki badań modelowych oraz analiza wpływu tarcia na stan obciążenia elementów łożysk hydrostatycznych. Przegląd Mechaniczny, nr 21.
5. Ivantysyn J., Ivantysynova M., 2001: Hydrostatic Pumps and Motors. Akadnia Books International, New Delhi.
6. Jerszow B. I., 1974: Oтыmajuščaja siła w torcowom zazorie niekatorych gidrawliczeskich ustrojstw. Wiestnik Maszynostrojenia, nr 5.
7. Jerszow B. I., Hiljuta I. M. Jerszow Sz. B., 1993: Ispytanie podpiatnikow aksjalnych maszyn. Wiestnik Maszynostrojenia, nr 1.
8. Kogl Ch., 1995: Versterbale hydrostatische Verdrangereinheiten im Drehzahl – und Drehmomentregelkreis am Netz mit angepaßtem Versorgungsdruck. Dissertation RWTH, Aachen.
9. Lachner H., 1974: Hydrostatische Lagerungen in Axialkolbenmasinen. Oldhydraulik und Pneumatik, nr 8.
10. Niegoda J., 1977: Badanie możliwości zastosowania tłoków z bezprzegubowym podparciem hydrostatycznym w pompach i silnikach wielotłoczkowych osiowych. Rozprawa doktorska, Politechnika Gdańska.
12. Osiecki A., 1998: Hydrostatyczny napęd maszyn. WNT, Warszawa.
13. Osiecki A., Osiecki L., 1998: Prace rozwojowe nad nową konstrukcją pomp wielotłoczkowych osiowych. Przegląd Mechaniczny, nr 4.
14. Osiecki L., 1998: Badanie zjawisk zachodzących w zespole tłoczek – stopka hydrostatyczna – dławik śrubowy maszyny wielotłoczkowej osiowej. Rozprawa doktorska, Politechnika Poznańska.
15. Osiecki A., Niegoda J., 1976: Tarcie w węźle tłoka maszyn wielotłoczkowych osiowych. Przegląd Mechaniczny nr 6.
16. Renius K.T., 1973: Experymentelle Untersuchungen an Gleitschuhen von Axialkolbenmaschinen. Olhydraulik und Pneumatik, 17 nr3.
17. Stryczek S., 1995: Napęd hydrostatyczny. WNT, Warszawa.
18. Szydelski Z., Olechowicz J., 1986: Elementy napędu i sterowania hydraulicznego i pneumatycznego. Warszawa.

OBCIĄŻENIE STOPEK HYDROSTATYCZNYCH MASZYN WIELOTŁOCZKOWYCH OSIOWYCH

Streszczenie. W opracowaniu przedstawiono analizę obciążenia stoppek hydrostatycznych występujących w maszynach wielotłoczkowych osiowych. Przykładowo opisano obciążenie podstawowych par kinematycznych pompy wielotłoczkowej osiowej. Przeanalizowano obciążenie jak i odciążenie hydrostatyczne stopki ze wskazaniem użycia podstawowych zależności matematycznych. Wyeksponowano graficznie rezultaty obliczeń symulacyjnych w programie MathCad momentu skręcającego stopkę podczas jej pracy w zależności od prędkości kątowej, ciśnienia roboczego masy stopki i współczynnika tarcia występującego pomiędzy stopką a tarczą pochyłą w przedziale strefy tłocznej.

Słowa kluczowe: pompa tłoczkowa, stopka hydrostatyczna, moment skręcający.